Eur. Phys. J. B (2013) 86: 54
DOI: 10.1140/epjb/e2012-30853-y

THE EUROPEAN PHYSICAL JOURNAL B

Regular Article

Sulfur dioxide adsorbed on graphene and heteroatom-doped graphene: a first-principles study

Li Shao, Guangde Chen, Honggang Ye[a], Yelong Wu, Zhijuan Qiao, Youzhang Zhu, and Haibo Niu

Department of Applied Physics and the MOE Key Laboratory for Nonequilibrium Synthesis and Modulation of Condensed Matter, Xi'an Jiaotong University, Xi'an, Shaanxi 710049, P.R. China

Received 19 September 2012 / Received in final form 14 December 2012
Published online 13 February 2013 –

Abstract. The adsorption of sulfur dioxide (SO_2) on intrinsic graphene and heteroatom-doped (B, N, Al, Si, Cr, Mn, Ag, Au, and Pt) graphene samples was theoretically studied using first-principles approach based on density functional theory to exploit their potential applications as SO_2 gas sensors. The structural and electronic properties of the graphene-molecule adsorption adducts are strongly dependent on the dopants. SO_2 molecule is adsorbed weakly on intrinsic graphene, and B-, N-doped graphene; in general, strong chemisorption is observed on Al-, Si-, Cr-, Mn-, Ag-, Au-, and Pt-doped graphene. The adsorption mechanisms are discussed from charge transfers and density of states. This work reveals that the sensitivity of graphene-based chemical gas sensors for SO_2 can be drastically improved by introducing appropriate dopant, and Cr, as well as Mn, may be the best choices among all the dopants.

1 Introduction

Graphene has attracted enormous scientific and technological interests in this novel single-carbon honeycomb atomic material since it was first discovered by Novoselov et al. in 2004 [1]. Its unique physicochemical properties, such as high surface area, excellent thermal and electric conductivity, and great mechanical strength, enable it with numerous potential applications, including composites [2], spin devices [3], solar cell technology [4], liquid crystal devices [5], and gas sensors [6]. Graphene-based nanostructures are believed to have a tremendous potential for developing sensors of various types. This is not only owing to the fact that graphene is a two-dimensional (2D) crystal with surface only and no volume, which maximizes the interaction between the surface dopants and adsorbates, but also due to the fact that a small change of carrier concentration can cause a notable variation of electrical conductivity. Besides, graphene could be deliberately or accidentally doped with noncarbon elements. Experimental and theoretical research have shown that graphene or heteroatom-doped graphene can be used as sensing materials to detect various gas molecules, such as O_2 [7–10], H_2 [11,12], CO [9,13–15], NH_3 [7,13,14,16], NO [10,13,14,16], NO_2 [7,9,13,14], N_2O [17], H_2O [9,14], HF [18], H_2CO [19] and so on. The sensitivity of CO, H_2O, and NH_3 up to 1ppb (parts per 10^9) was demonstrated and even can detect a single molecule for NO_2 in future [20].

Sulfur dioxide (SO_2) is a colorless gas and can be used as preservative, bleach, fungicide, and raw material of preparation of H_2SO_4. But SO_2 is also one of the main pollutants with toxicity released into the atmosphere as a result of the burning of sulfur bearing fossil fuels in automobile engines, industrial complexes, power plants, and house-holds [21]. The subsequent interaction of the SO_2 with air results in the formation of "acidic rains", which can make rivers and lakes acidize, destroy soil, vegetation, forests and corrode metals and buildings. A great amount of efforts has been devoted to find an effective technique for SO_2 detection. The sensitivity of graphene or doped graphene to SO_2 may provide new insights into the development of next generation gas sensors for virtual applications.

In this work, the adsorptions of SO_2 on intrinsic graphene (IG) and B-, N-, Al-, Si-, Cr-, Mn-, Ag-, Au-, Pt-doped graphene (BG, NG, AlG, SiG, CrG, MnG, AgG, AuG, PtG) have been investigated by performing ab initio calculations. The model systems are carefully chosen to cover several basic issues. The most stable adsorption configurations, adsorption energies, charge transfers, and density of states (*DOS*) of the systems were calculated and analyzed. The motivation of this paper is to exploit the potential applications of graphene as gas sensor.

2 Computational methods

The spin-polarized density functional theory (DFT) calculations were performed with the Vienna ab initio simulation package (VASP) [22,23] using the generalized gradient

[a] e-mail: hgye@mail.xjtu.edu.cn

approximation (GGA) with PW91 function [24] for the exchange and correlation effects of the electrons. As is known, the equilibrium distance between adsorbate and the graphene sheet will be somewhat overestimated and consequently the binding energy will be underestimated in GGA, but valuable results still can be obtained within this frame. It has been widely used to study the doping and adsorption of graphene [14,15,17]. Electron-ion interactions were described by the projector-augmented wave (PAW) method, which is basically a frozen-core all-electron calculation [25]. The energy cut-off is taken to be 400 eV and the k-point is set to $3 \times 3 \times 1$ for the Brillouin-Zone (BZ) integration in structure optimization. The mesh of **K** space is increased to $9 \times 9 \times 1$ to obtain accurate electronic structures and the density of states (DOS). Each simulated system under investigation consists of a 14.78 Å × 14.78 Å × 20 Å graphene supercell (6×6 unit cell) with a single SO_2 molecule adsorbed in the central region. The distance between adjacent graphene layers was kept as 20 Å, which is sufficient to minimize the interaction between them. In optimizing atomic structures, the force convergence criterion was set to 0.03 eV/Å. The adsorption energy, E_{ad}, is defined as

$$E_{ad} = E_{sheet} + E_{SO_2} - E_{total} \quad (1)$$

where E_{sheet}, E_{SO_2}, and E_{total} are the energies of the isolated graphene sheet, the isolated SO_2 molecule, and the relaxed graphene sheet with an adsorbed SO_2 molecule, correspondingly. To find out the most stable adsorption configuration of SO_2 on IG and XG (X represents the dopants), several different initial positions and orientations of SO_2 molecule above each graphene sheet were considered.

3 Results and discussion

As a preliminary test, we optimized the atomic geometries of SO_2 gas molecule, IG, and XG using the aforementioned DFT method. The bond length and bond angle of SO_2 molecule in ground state are 1.454 Å and 119.216°, which are in good agreement with experimental values (1.43 Å and 119.5°, respectively). The calculated C-C bond length in graphene is 1.422 Å, which is consistent with the experimental value (1.42 Å), as well.

Firstly, we focused on the SO_2 adsorbed on IG, BG and NG. Figure 1 shows the most stable adsorption configurations of SO_2 molecule on IG and BG (the case of NG is the same as BG), i.e. the configurations with lowest-energy among various adsorption sites. More detailed information, such as absorption energy E_{ad}, distance between adjacent atoms d (defined as the center-to-center distance of nearest atoms), the bond angle Ø(O-S-O) and the charge transfer Q (Bader charge [26]) are listed in Table 1.

From Figure 1 and Table 1, we can see that the most energetically favorable configuration of SO_2 adsorbed on IG is the one with S atom almost on the top of one C atom (Fig. 1a). The calculated E_{ad} is 0.012 eV and the molecule-sheet distance (d) is 3.279 Å. The longer S-O bond length

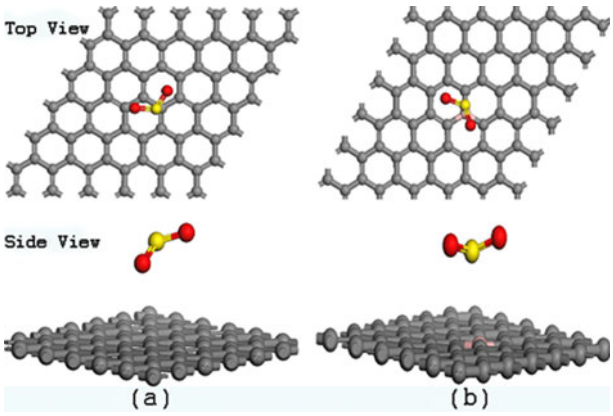

Fig. 1. (Color online) The most stable adsorption configurations of SO_2 molecule on IG (a) and BG (b). Gray, pink, red, and yellow spheres denote C, B, O, and S atoms, respectively.

and bond angle Ø(O-S-O) are 1.459 Å and 118.743°, respectively, which almost remain the values as in gas phase (1.454 Å and 119.216°, respectively). All of these indicate that the SO_2 undergoes weak adsorption on IG, which is in agreement with the results of other small molecules adsorbed on IG [7–9,13,18].

As for BG and NG, there is no obvious local distortion in graphene when B and N are doped because of B and N being the nearest elements with C in the periodic table, i.e. their atomic radii are close to C. Take BG for example, we found that the most favorable structure of SO_2 adsorbed on BG is the configuration with S atom almost on top of B (Fig. 1b). From Table 1, we can learn that E_{ad} is too small (0.205 eV) and d is too large (3.162 Å), indicating nonstable adsorption of SO_2 molecule on BG. Similar results can be found for NG.

When SO_2 molecule is adsorbed on large element doped graphenes, two different fully optimized configurations for AlG, SiG, PtG, and three for CrG, MnG, AgG, and AuG can be found. In Figure 2, we present the three stable adsorption configurations of SO_2 molecule on MnG, which is a typical representative. From the figure, we can see that the SO_2 molecule can bond to the doped graphene by the S atom or one O atom or both of them. The adsorption energies of these obtained structures for different dopants are shown in Table 2, suggesting that, for most of them, the structure both bonded by S and O atoms is the most stable one, as it has the largest E_{ad} among the three obtained structures for each of these large element doped graphene. More detailed information for the most stable adsorption configurations can be found in Table 1. The net charge transfer (Q) from the graphene sheet to SO_2 molecule is calculated by Bader analysis of the charge distribution to understand the change of electronic structures in graphene caused by the physi- or chemisorption of adsorbate. Note that in Table 1, only $Q = 0.744$ and 0.959 e for AlG and SiG, respectively, from graphene to SO_2 molecule are larger than $Q = 0.672$ and 0.599 e for CrG and MnG, the other cases are smaller than them. Large charge transfer for CrG and MnG causes

Table 1. Adsorption energy E_{ad} (eV), bond angle Ø(O-S-O) (°), distance between adjacent atoms d (Å), and Bader charge Q (e) for the most stable adsorption configurations of SO_2 on IG and XG[1].

	IG	BG	NG	AlG	SiG	PtG	MnG	CrG	AgG	AuG
E_{ad} (eV)	0.012	0.205	0.172	1.262	0.902	1.018	1.729	1.675	0.968	1.284
Ø(O-S-O)(°)	118.743	118.294	117.177	113.357	111.002	114.856	114.204	113.409	115.232	114.626
d_{S-O}[2] (Å)	1.459	1.460	1.476	1.566	1.627	1.566	1.584	1.585	1.543	1.581
d_{X-C}[3] (Å)		1.486	1.409	1.899	1.774	1.944	1.805	1.853	2.093	2.145
d_{S-M}[4] (Å)	3.279	3.162	3.478	1.825	1.737	2.229	1.905	1.927	2.173	2.167
Q[5] (e)	–0.077	–0.110	–0.263	–0.744	–0.959	–0.550	–0.599	–0.672	–0.454	–0.479

[1] X represents the dopants. [2] The longer S-O bond length of SO_2 molecule. [3] The nearest distance among X and three adjacent C atoms. [4] The nearest distance among graphene sheet and the three atoms of SO_2 molecule. [5] A negative number means charge transfer from graphene to SO_2 molecule.

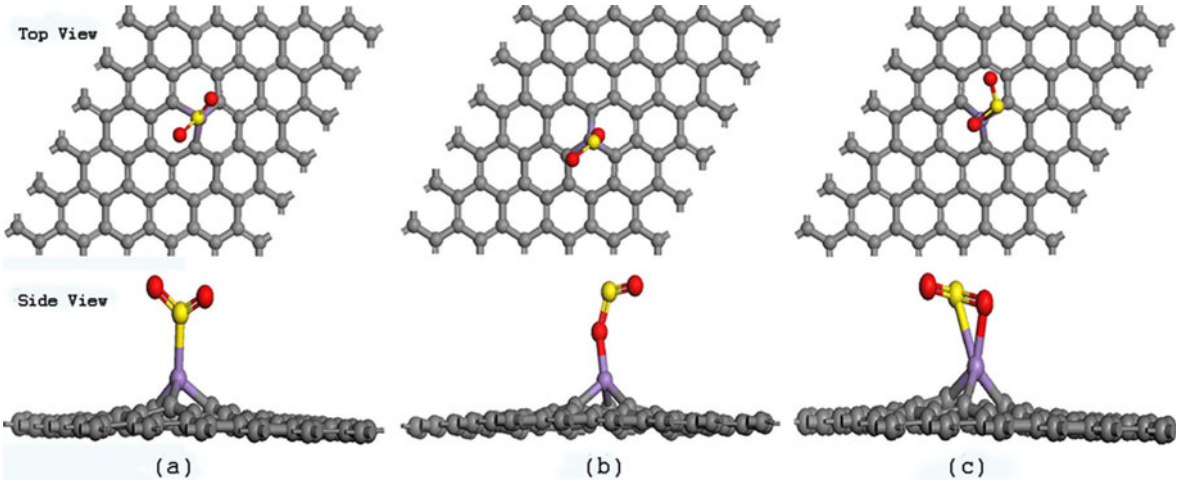

Fig. 2. (Color online) The three stable adsorption configurations of SO_2 molecule on MnG with Mn atom bonded to S atom (a), O atom (b), and S, O atoms (c). Gray, brown, red, and yellow spheres denote C, Mn, O and S atoms, respectively.

Table 2. Adsorption energies E_{ad} (eV) of obtained structures for different dopants.

	S, O[1]	O	S	Nonbonding
AlG		1.262		0.313
SiG		0.902	0.275	
PtG	1.108	0.788		
CrG	1.675	1.583	1.147	
MnG	1.729	1.624	1.142	
AgG	0.968	0.845	0.716	
AuG	1.284	0.901	1.006	

[1] The atom(s) of SO_2 molecule bonded to the dopant.

significant change of the atomic geometry of SO_2 (Tab. 1) which results in very strong adsorption and large adsorption energy. Large charge transfer also suggests that SO_2 molecule is chemically adsorbed on CrG and MnG. We can infer that it is physisorption between SO_2 and IG, BG, and NG. Furthermore, the adsorption energy of CrG and MnG is larger than that in other cases. As a whole, Cr and Mn are more appropriate dopants for SO_2.

The electronic density difference images confirm the Bader analysis results. Figure 3 shows the electronic density difference of SO_2 on CrG and MnG, for the sake of comparison, the result of SO_2 on BG is also presented. The blue and yellow regions denote the areas of electron accumulation and the electron loss, respectively. No charge accumulation can be seen between BG and SO_2 molecule from Figure 3a, which indicates that the interaction between SO_2 molecule and BG are of weak physisorption once again. However, Figures 3b and 3c show that there are charge redistribution between SO_2 molecule and CrG and MnG. The three atoms of SO_2 gain electrons from the CrG and MnG, which demonstrates that the charge transfers will form ionic bond(s) between the atom(s) of SO_2 and the Cr and Mn, with the SO_2 molecule acting as the electron acceptor of the systems. As the plenty of charge accumulation between the SO_2 and CrG and MnG, it is expected to bring significant change to the electronic properties of the graphene sheets.

To have a further insight into the effect of SO_2 adsorption on the electronic structure, the spin-polarized total density of states (DOS) and projected density of states ($PDOS$) of IG and XG without and with adsorbed SO_2 were calculated. The DOS and $PDOS$ for some representative systems are shown in Figure 4. For BG the contribution from SO_2 is localized between –7 and –2.5 eV in the valence bands and around 1.2 eV in the conduction bands (Fig. 4a), which are far away from the Fermi

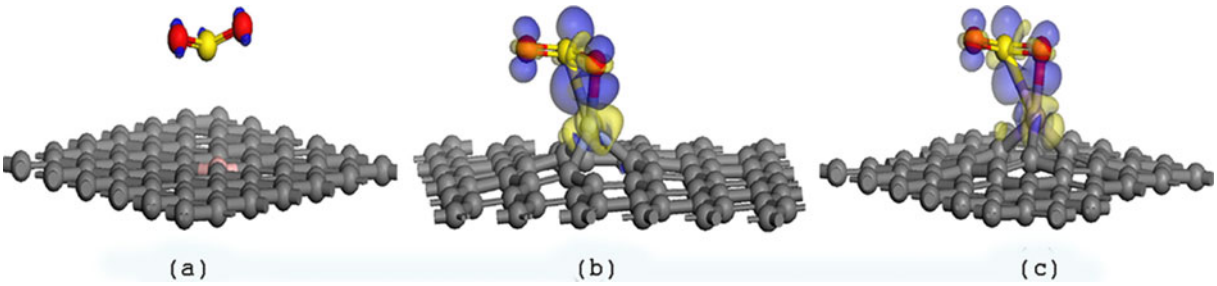

Fig. 3. (Color online) The electronic density difference images for the adsorption of SO_2 on BG (a), CrG (b), and MnG (c). Charge accumulation is in blue and depletion in yellow. The isosurface is ± 0.03 e/Å^3.

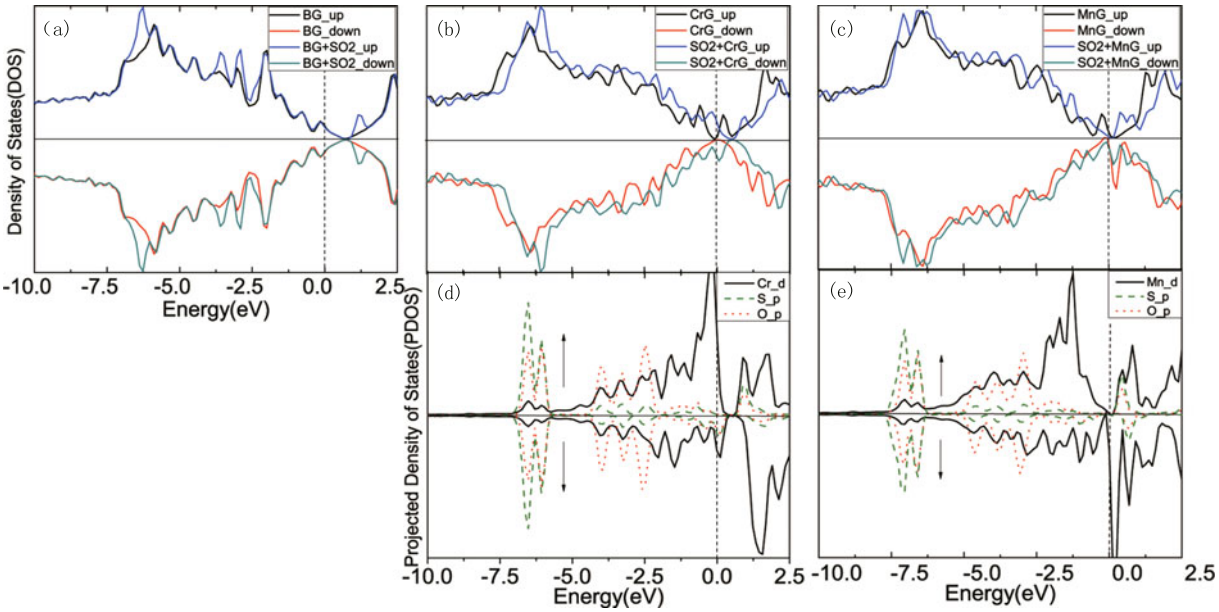

Fig. 4. (Color online) Total density of states (*DOS*) of BG (a), CrG (b), and MnG (c) before and after the adsorption of SO_2 molecule and projected *DOS* for $SO_2 + CrG$ (d) and $SO_2 + MnG$ (e). The atom of *PDOS* of O_p is the one which bonds to X (X = Cr, Mn) atom. The arrows denote the spin-up (↑) states and spin-down (↓) states. The Fermi level is set to zero.

level, E_f. The *DOS* near E_f has no distinct change and the conductivity change is barely observable, indicating that the BG is not sensitive for the presence of SO_2 molecule. On the contrary, adsorption of SO_2 onto the CrG and MnG causes the major band features to move towards higher energy, i.e. E_f shifts towards lower energy. For $SO_2 + CrG$ (Figs. 4b and 4d), not only the *DOS* near E_f for spin down appears a new peak, but also the peak for spin up shifts to higher energy, suggesting that the conductivity of graphene sheet would increase remarkably upon exposure to SO_2. Comparison of the *PDOS* of adsorbed SO_2 with the *DOS* of $SO_2 + CrG$ reveals that the *DOS* at E_f are mainly contributed by the $3d$ electrons in Cr atom hybridizing with $2p$ electrons in S, O atoms which bond to Cr. The similar phenomena, which are in reasonable agreement with our analysis above, also have been observed in MnG (Figs. 4c and 4e). As a result, the chemisorbed SO_2 on CrG and MnG will give rise to a large change in the electrical conductivity of the doped graphene layers. Therefore, CrG and MnG can be used to detect this toxic molecule by detecting the conductivity change before and after the adsorption of SO_2.

4 Conclusion

Via ab initio simulations we have thoroughly investigated the adsorption of SO_2 molecule on IG and XG (X = B, N, Al, Si, Cr, Mn, Ag, Au, and Pt). Our calculations indicate that intrinsic graphene is not an efficient material to capture SO_2, and B-, N-doped graphene are not sensitive for SO_2 molecule because of weak adsorption. In general, Al-, Si-, Ag-, Au-, Pt- especially Cr- and Mn-doped graphene can adsorb SO_2 molecule strongly on the surfaces. The elongations of S-O bond, the decreases of bond angle Ø(O-S-O), the short distances between SO_2 molecule and the graphene sheet, the big adsorption energies, the relatively large charge transfers to SO_2 molecule, the obvious electronic density difference images, and the changes of *DOS* before and after the adsorption of SO_2 molecule support

that Cr- and Mn-doped graphene can be more suitable for the detection of SO_2 gas. It is expected that the above results may foster the industrial applications of graphene sensors.

This work is supported by the National Natural Science Foundation of China under Grant Nos. 11074200, 61176079, and 11204231.

References

1. K.S. Novoselov, A.K. Geim, S.V. Morozov, D. Jiang, Y. Zhang, S.V. Dubonos, I.V. Grigorieva, A.A. Firsov, Science **306**, 666 (2004)
2. W. Supinda, A.D. Dmitriy, S. Sasha, P. Richard, J. Inhwa, H.B.D. Geoffrey, E. Guennadi, W. Shang-En, C. Shu-Fang, L. Chuan-Pu, T.N. SonBinh, S.R. Rodney, Nano Lett. **7**, 1888 (2007)
3. T. Nikolaos, J. Csaba, P. Mihaita, T.J. Harry, J. van Wees Bart, Nature **448**, 571 (2007)
4. Wang Xuan, Zhi Linjie, M. Klaus, Nano Lett. **8**, 323 (2007)
5. B. Peter, D.B. Paul, R.N. Rahul, J.B. Tim, J. Da, S. Fred, A.P. Leonid, V.M. Sergey, F.G. Helen, W.H. Ernie, K.G. Andre, S.N. Kostya, Nano Lett. **8**, 1704 (2008)
6. I.I. Barbolina, K.S. Novoselov, S.V. Morozov, S.V. Dubonos, M. Missous, A.O. Volkov, D.A. Christian, I.V. Grigorieva, A.K. Geim, Appl. Phys. Lett. **88**, 013901 (2006)
7. Miao Zhou, Yun-Hao Lu, Yong-Qing Cai, Chun Zhang, Yuan-Ping Feng, Nanotechnology **22**, 385502 (2011)
8. Dai Jiayu, Yuan Jianmin, Phys. Rev. B **88**, 165414 (2010)
9. Y. Zou, F. Li, Z. Zhu, M. Zhao, X. Xu, X. Su, Eur. Phys. J. B **81**, 475 (2011)
10. Pramanik Anup, Kang Hong Seok, J. Phys. Chem. C **115**, 10971 (2011)
11. Choi Woon Ih, Jhi Seung-Hoon, Kim Kwiseon, Kim Yong-Hyun, Phys. Rev. B **81**, 085441 (2010)
12. E. Rangel, J.M. Ramirez-Arellano, I. Carrillo, L.F. Magana, Int. J. Hydrogen Energy **36**, 13657 (2011)
13. Zhang Yonghui, Chen Yabin, Zhou Kaige, Liu Caihong, Zeng Jing, Zhang Haoli, Peng Yong, Nanotechnology **20**, 185504 (2009)
14. O. Leenaerts, B. Partoens, F.M. Peeters, Phys. Rev. B **77**, 125416 (2008)
15. Z.M. Ao, J. Yang, S. Li, Q. Jiang, Chem. Phys. Lett. **461**, 276 (2008)
16. A. Saffarzadeh, J. Appl. Phys. **107**, 114309 (2010)
17. Lv Yong-An, Zhuang Gui-Lin, Wang Jian-Quo, Jia Ya-Bo, Xie Qin, Phys. Chem. Chem. Phys. **13**, 12472 (2011)
18. Sun Yuanyuan, Chen Li, Zhang Feiwu, Li Daoyong, Pan Hongzhe, Ye Jun, Solid State Commun. **150**, 1906 (2010)
19. Qin Xian, Meng Qingyuan, Zhao Wei, Surf. Sci. **605**, 930 (2011)
20. F. Schedin, A.K. Geim, S.V. Morozov, E.W. Hill, P. Blake, M.I. Katsnelson, K.S. Novoselov, Nature Mater. **6**, 652 (2007)
21. Kh. M. Eid, H.Y. Ammar, Appl. Surf. Sci. **257**, 6049 (2011)
22. G. Kresse, J. Hafner, Phys. Rev. B **47**, 558 (1993)
23. G. Kresse, J. Furthmüller, Phys. Rev. B **54**, 11169 (1996)
24. J.P. Perdew, Y. Wang, Phys. Rev. B **45**, 13244 (1992)
25. G. Kresse, D. Joubert, Phys. Rev. B **59**, 1758 (1999)
26. H. Graeme, A. Andri, J. Hannes, Comput. Mater. Sci. **36**, 354 (2006)